Electron heating in high Mach number collisionless shocks

Arno Vanthieghem

SF2A 2024
Marseille
June 4-7, 2024

Based on

AV, V. Tsiolis, A. Spitkovsky, Y. Todo, K. Sekiguchi, F. Fiuza, Phys. Rev. Lett. (2024)

AV, M. Lemoine, L. Gremillet, ApJ Lett. (2022)

In collaboration with

V. Tsiolis (Princeton U.)
A. Spitkovsky (Princeton U.)
F. Fiuza (IST)
Y. Todo (NIFS)
M. Lemoine (IAP)
L. Gremillet (CEA)
K. Sekiguchi (NAOJ)

Magnetization and shock speed are key parameters to characterize the shock physics

$$\sigma \equiv \frac{B^2}{4\,\pi(\gamma-1)n\,m\,c^2}$$

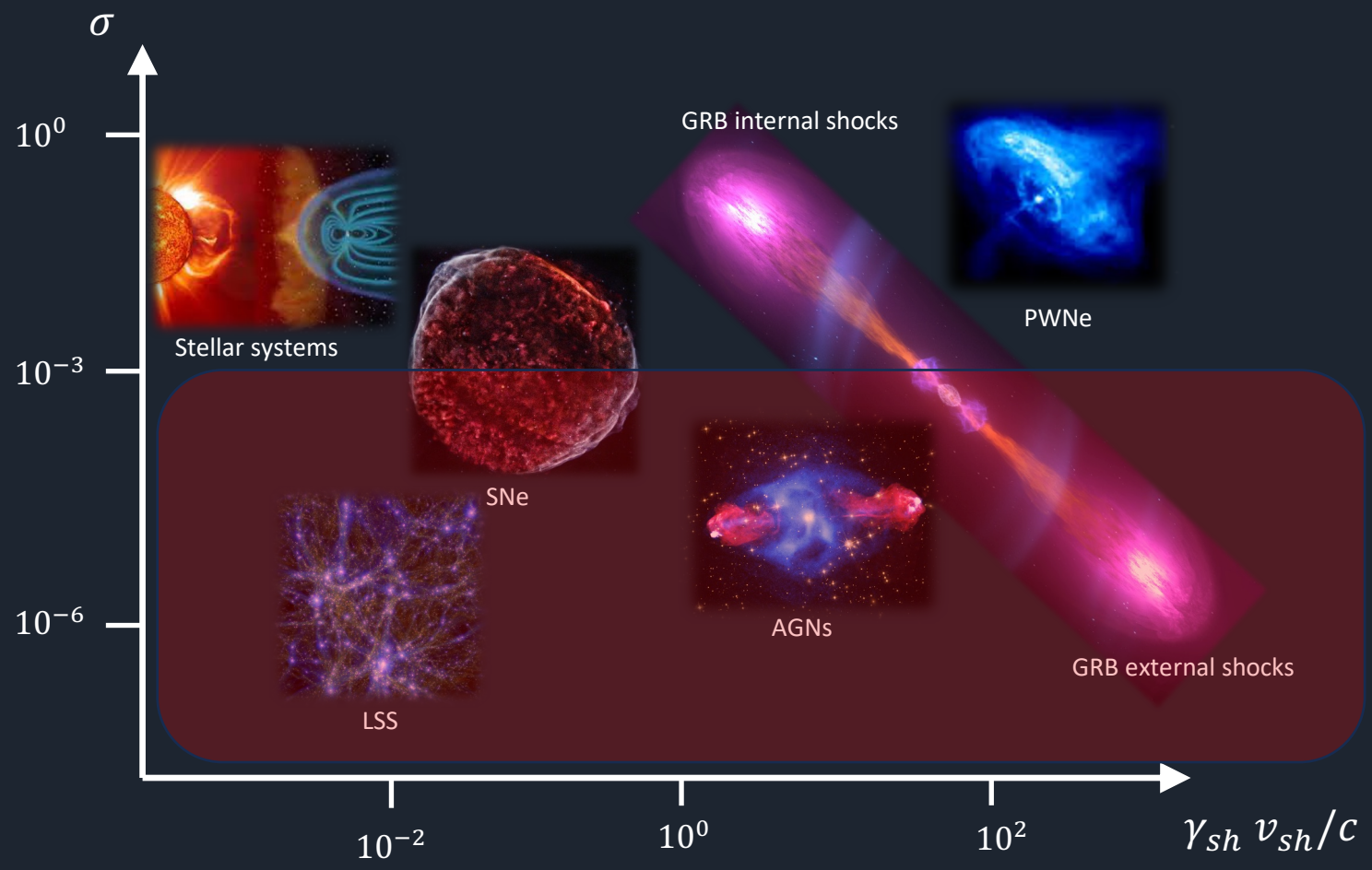

Weakly magnetized shocks are dominated by magnetic modes advected towards the shock by the bulk plasma flow

$M_A \gg 100$

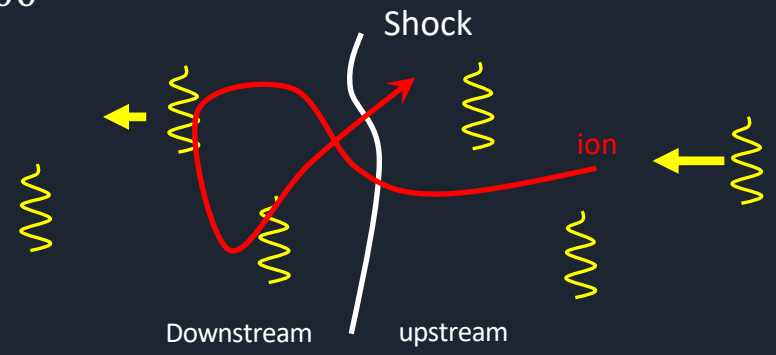

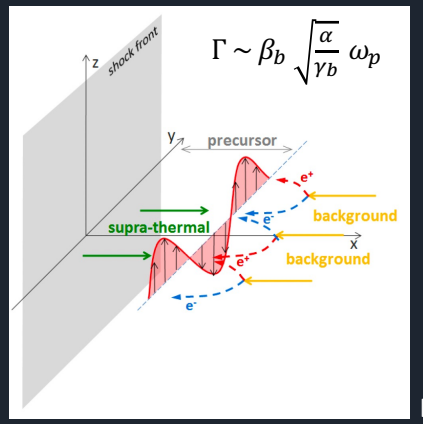

Dominant instability

Plasma is coupled through the Weibel instability from the interplay between the background plasma and accelerated particles

Bret et al., 2010, Pelletier et al., 2017

with a transition to larger scale modes …

Weibel, 1956, Brendan et al., 1975, Medvedev & Loeb, 1999

High Alfvén Mach number collisionless blast waves efficiently heat electrons

- SNR shock waves observations[1,2] & in-situ measurements[3]

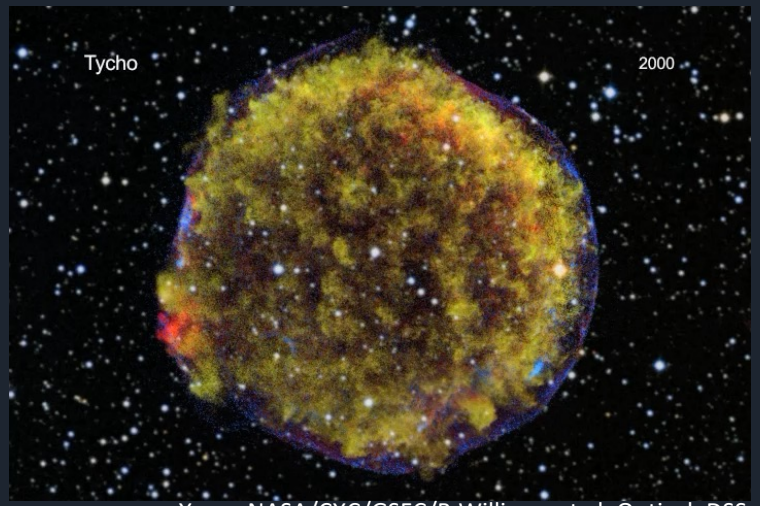

X-ray: NASA/CXC/GSFC/B.Williams et al; Optical: DSS

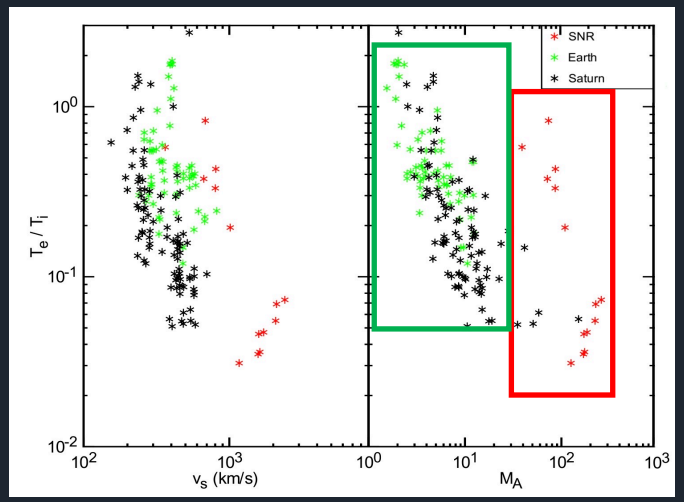

P. Ghavamian et al Space Sci. Rev. 178, 633 (2013)

[1]P. Ghavamian et al SSR (2013)

[2]J. Raymond et al., ApJ (2023)

[3]A. Johlander et al., GRL (2023)

[4]T. Kato & H. Takabe, ApJL (2008)

[5]T. Amano et al., ApJ (2009)

[6]T. Kato & H. Takabe, ApJ (2010)

[7]A. Bohdan et al., PRL (2021)

High Alfvén Mach number collisionless blast waves efficiently heat electrons

- SNR shock waves observations[1,2] & in-situ measurements[3]

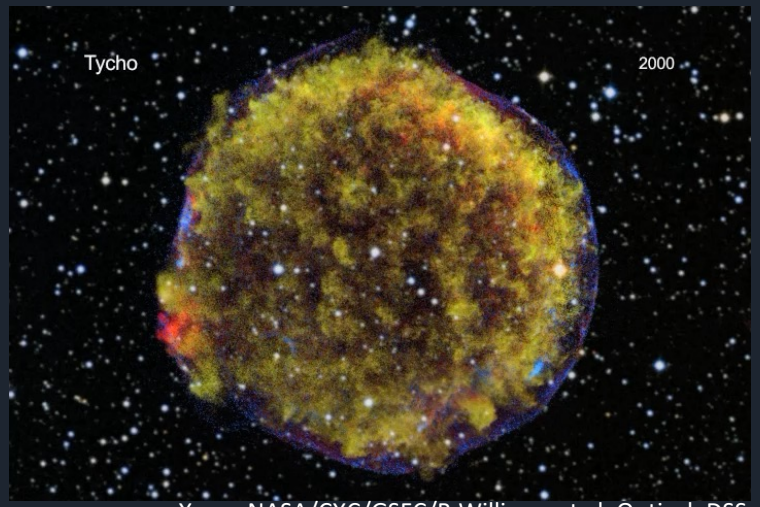

X-ray: NASA/CXC/GSFC/B.Williams et al; Optical: DSS

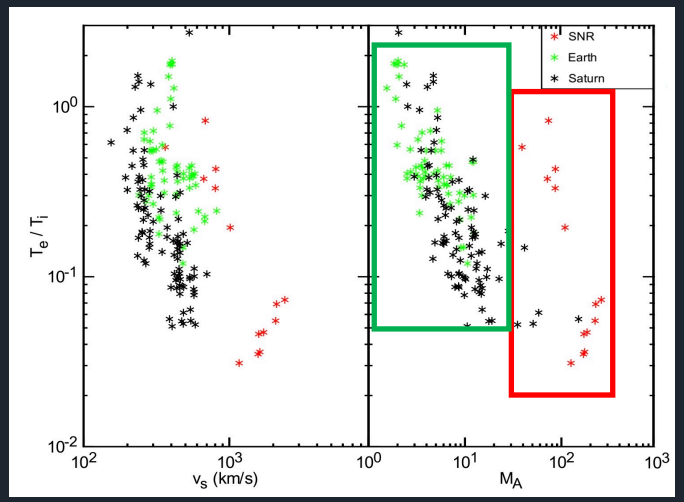

P. Ghavamian et al Space Sci. Rev. 178, 633 (2013)

- Kinetic simulations[4,5,6]

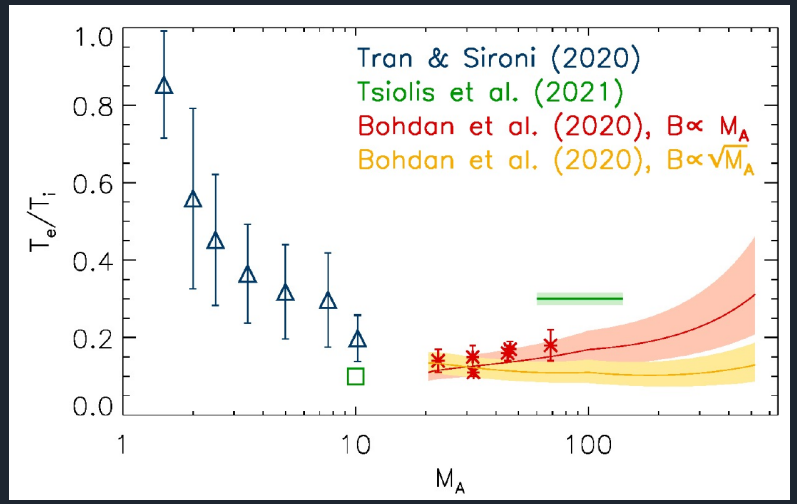

J. Raymond et al., ApJ 959, 50 (2023)

[1]P. Ghavamian et al SSR (2013)
[2]J. Raymond et al., ApJ (2023)
[3]A. Johlander et al., GRL (2023)
[4]T. Kato & H. Takabe, ApJL (2008)
[5]T. Amano et al., ApJ (2009)
[6]T. Kato & H. Takabe, ApJ (2010)
[7]A. Bohdan et al., PRL (2021)

High Alfvén Mach number collisionless blast waves efficiently heat electrons

- SNR shock waves observations[1,2] & in-situ measurements[3]

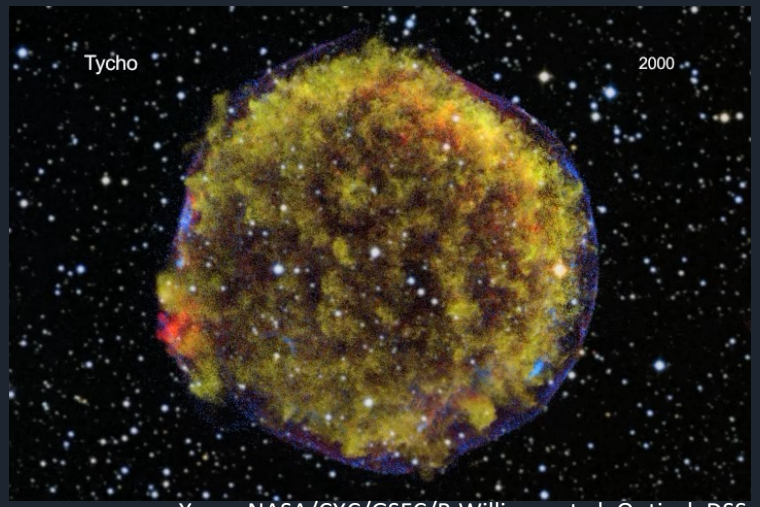

X-ray: NASA/CXC/GSFC/B.Williams et al; Optical: DSS

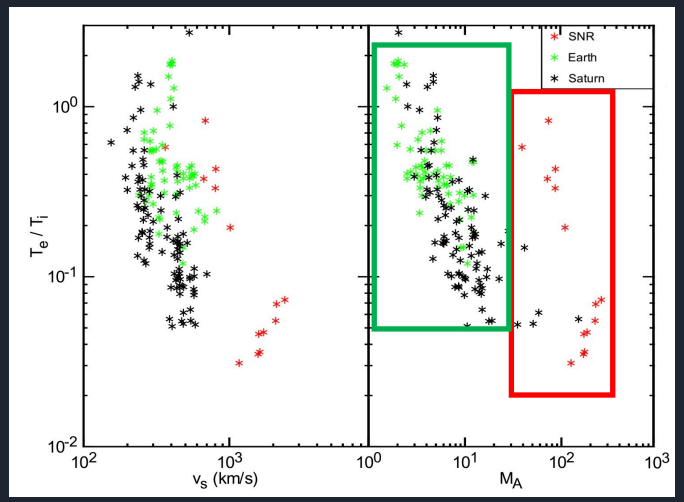

P. Ghavamian et al Space Sci. Rev. 178, 633 (2013)

- Kinetic simulations[4,5,6]

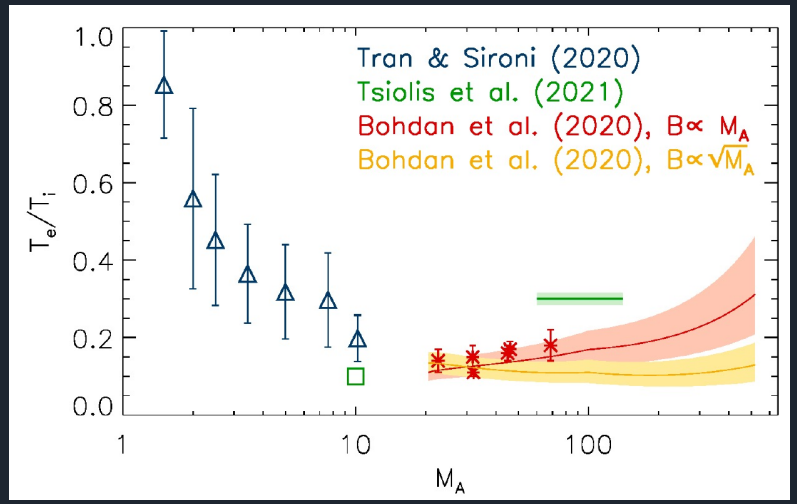

J. Raymond et al., ApJ 959, 50 (2023)

- Laboratory experiments

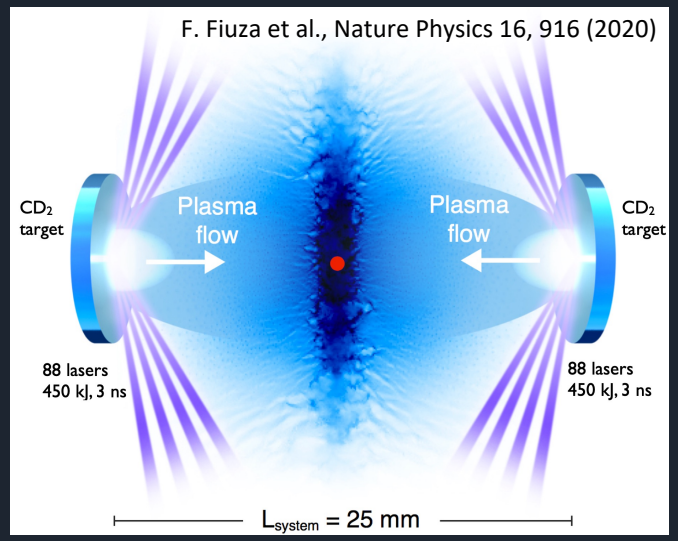

Efficient collisionless electron heating demonstrated at NIF

$$\frac{Z\,T_e}{T_i} = 0.24 - 0.45$$

[1]P. Ghavamian et al SSR (2013)
[2]J. Raymond et al., ApJ (2023)
[3]A. Johlander et al., GRL (2023)
[4]T. Kato & H. Takabe, ApJL (2008)
[5]T. Amano et al., ApJ (2009)
[6]T. Kato & H. Takabe, ApJ (2010)
[7]A. Bohdan et al., PRL (2021)

The turbulence is magnetically dominated, and drifts close to the electron bulk velocity

The scattering center frame (Weibel frame $\mathcal{R}_w$)

- The precursor of the shock is dominated by the Weibel instability

$$\Rightarrow \boldsymbol{E}^2 - \boldsymbol{B}^2 < 0$$

- At each point, one can define a local quasi-magnetostatic reference frame $\mathcal{R}_w$ [1,2]

$$\Rightarrow u_w \sim \frac{E\times B}{B^2} \sim \frac{\omega}{k}\frac{\epsilon_{xy}}{\epsilon_{yy}} \sim u_e$$

- Electrons drift close to the Weibel frame in the shock precursor

[1]C. Ruyer et al PRL 117, 065001 (2016) [2]G. Pelletier et al PRE 100, 013205 (2019)

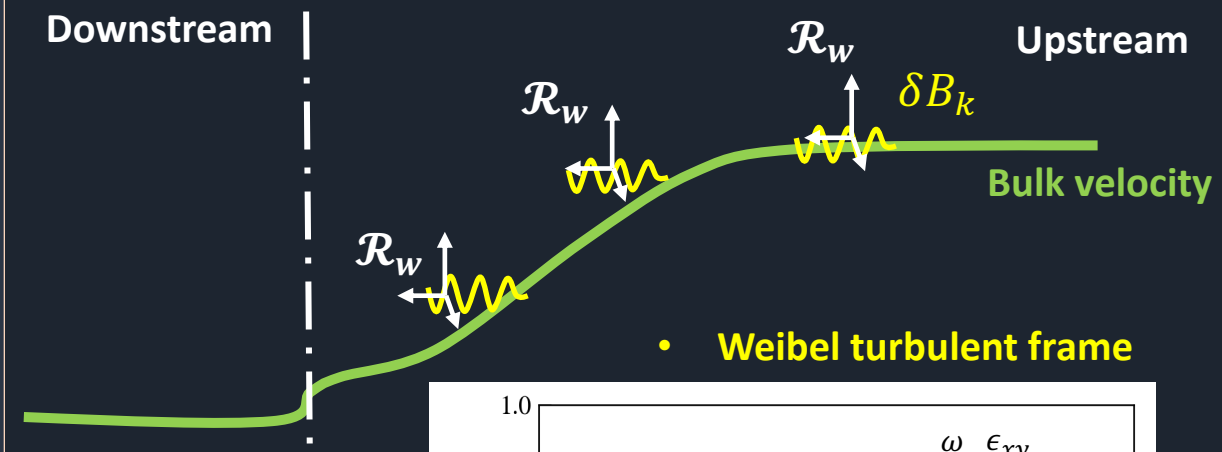

- **Weibel turbulent frame**

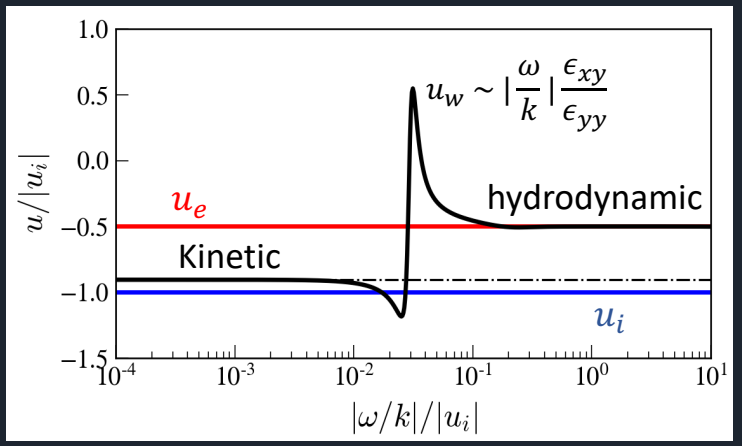

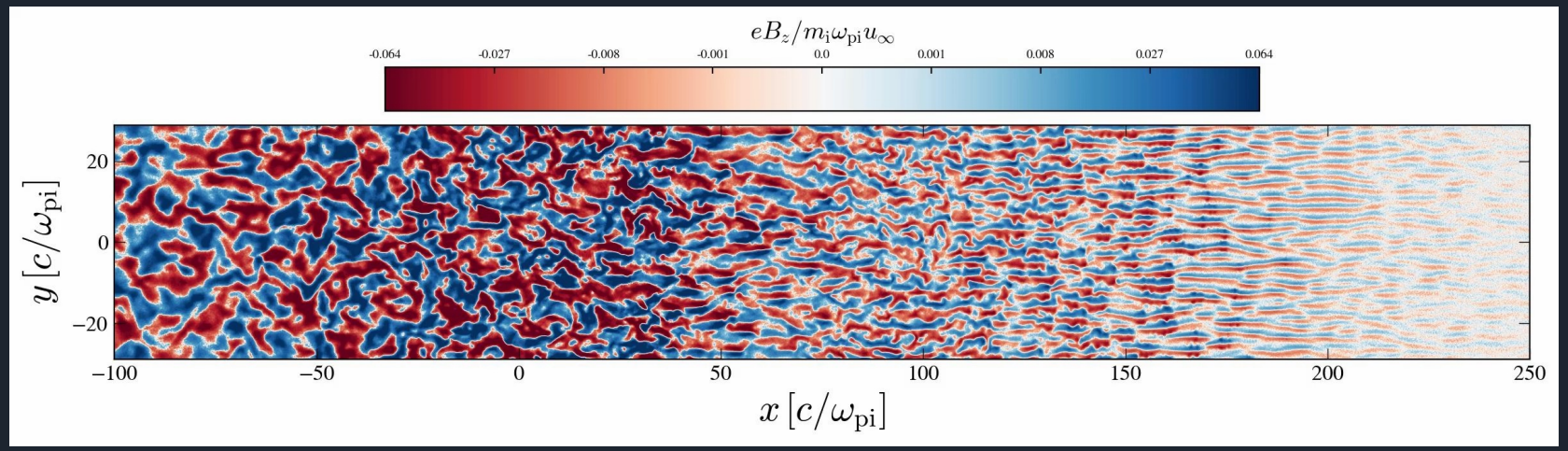

- $u_{sh} = 0.075$;
- $\Delta x = 0.1\frac{c}{\omega_{pe}}$;
- $c\Delta t = 0.45\,\Delta x$;
- 32 ppc;
- $m_i = 49\ m_e$

Tristan-mp

AV, V. Tsiolis et al., PRL (2024)

Energy partition through Joule heating in the ambipolar electric field resulting from effective scattering in a decelerating microturbulence

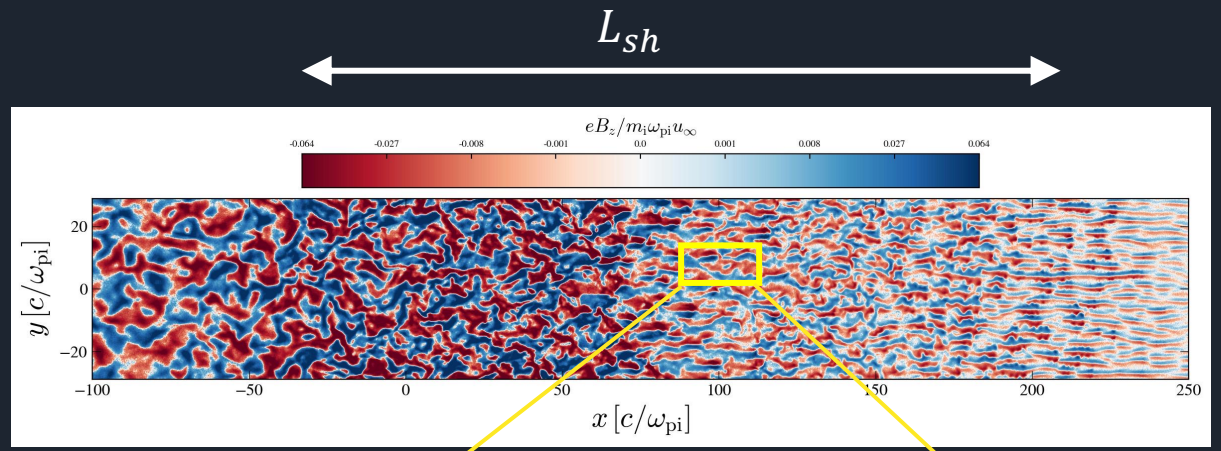

$u_{sh} = 0.075; \Delta x = 0.1\frac{c}{\omega_{pe}}; c\Delta t = 0.45\,\Delta x$; 32 ppc; $m_i = 49\,m_e$ (Tristan-mp)

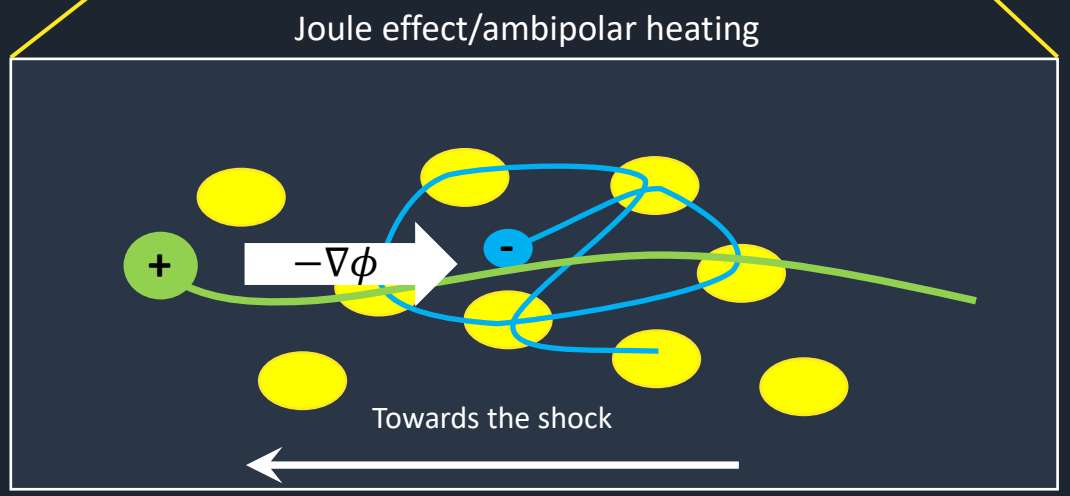

Model

- Collisionless friction with a magnetized microturbulence
- Electrostatic field from charge separation in a decelerated plasma

Equation of motion in the turbulence frame (Weibel frame $\boldsymbol{u_w}$)

$$\dot{\boldsymbol{p}} = \boldsymbol{p}\cdot\delta\hat{\boldsymbol{\Omega}}_t + q\,\boldsymbol{E} - m\,\dot{\boldsymbol{u}}_w$$

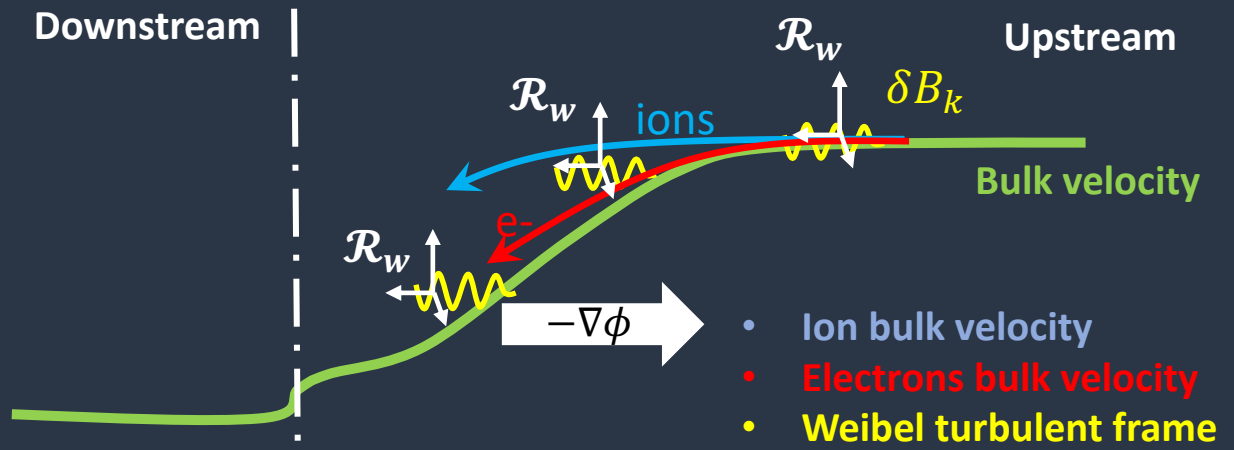

AV, V. Tsiolis et al., PRL (2024)

Small angle scattering for the weakly magnetized ions

Ion scattering frequency

$$\nu \sim \Delta\theta^2/\Delta t$$

Small angle pitch-angle scattering

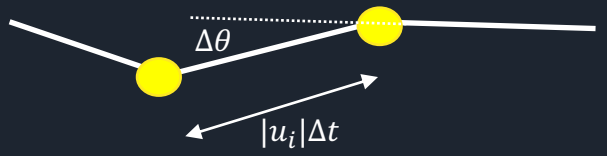

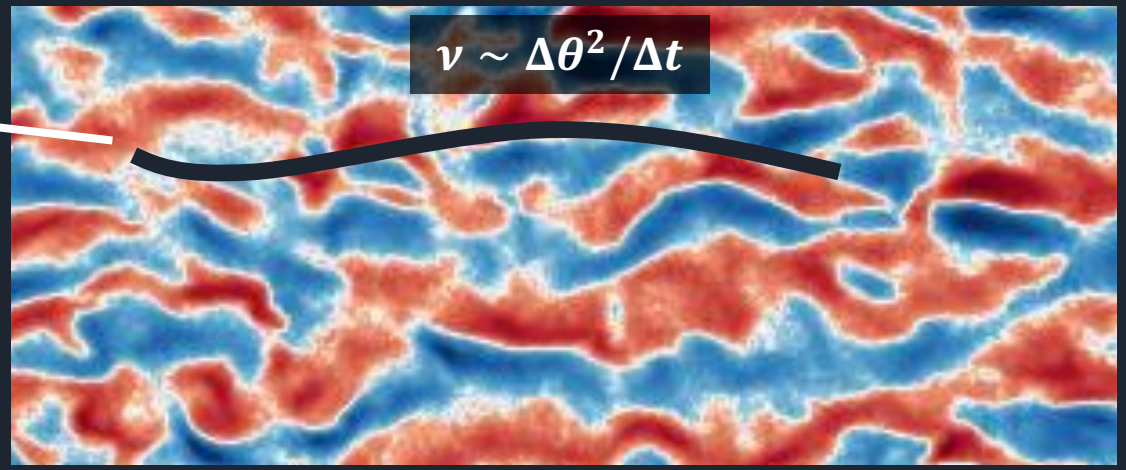

Magnetic field profile

- Small angle scattering
  $\Delta\theta^2 \sim r_\perp^2/r_{g,i}^2$
- Scattering time
  $\Delta t \sim \dfrac{r_\perp}{|u_{sh}|}$

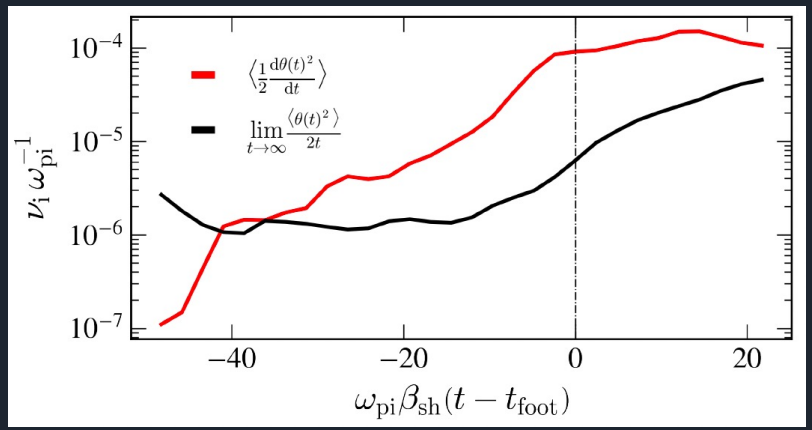

Tracked particles

$$L_{sh} \sim 10^2 \frac{c}{\omega_{pi}} \qquad u_{sh} = 0.075\,c$$

$$k_\perp \sim \omega_{pi}/c \qquad \Rightarrow \boldsymbol{\nu_i \sim 10^{-4}\omega_{pi}}$$

$$\nu_i \sim \frac{r_\perp |u_{sh}|}{r_{g,i}^2}$$

AV, V. Tsiolis et al., PRL (2024)

Strongly magnetized electrons scatter through decoherence of the betatron motion in the finite filaments

$\nu \sim \Delta\theta^2/\Delta t$

Ion scattering frequency

Small angle pitch-angle scattering

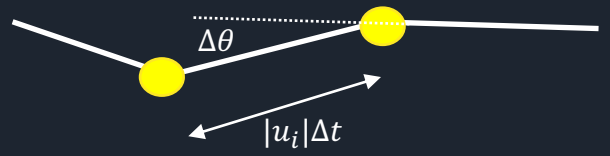

- Small angle scattering $\Delta\theta^2 \sim r_\perp^2/\mathrm{r}_{\mathrm{g,i}}^2$
- Scattering time $\Delta t \sim \dfrac{r_\perp}{|u_{\mathrm{sh}}|}$

$$\nu_i \sim \frac{r_\perp |u_{\mathrm{sh}}|}{r_{g,i}^2}$$

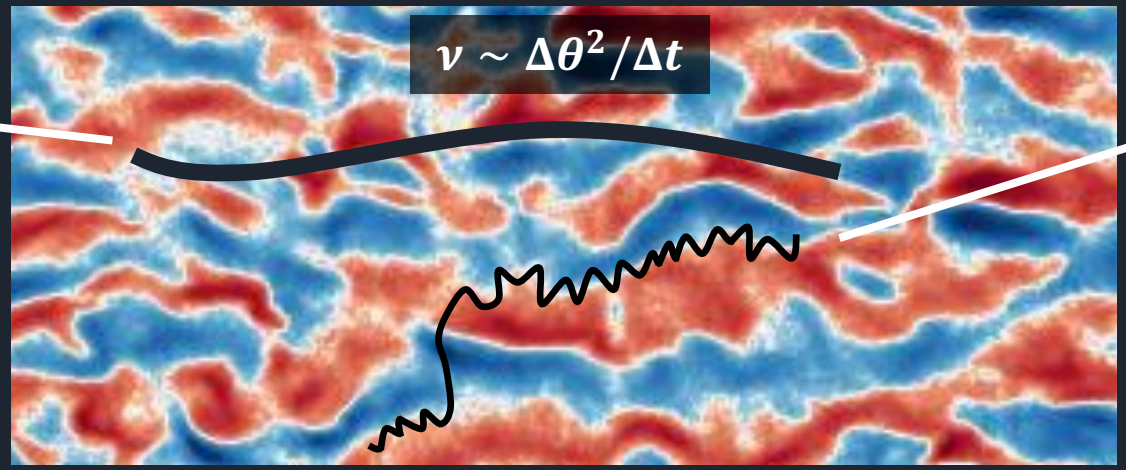

Magnetic field profile

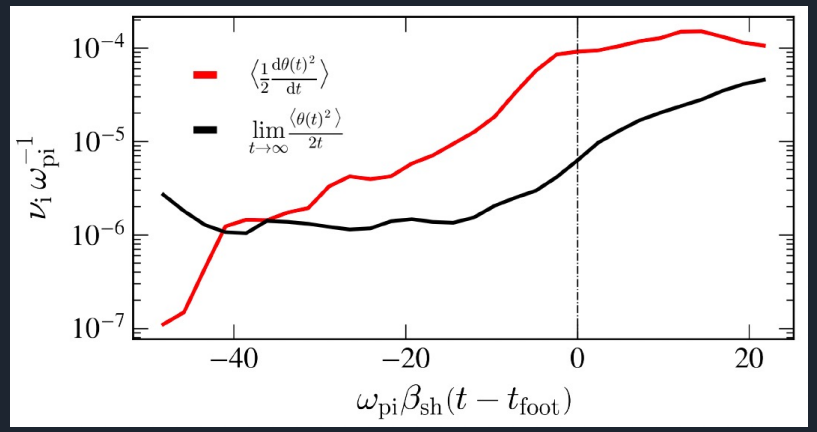

Tracked particles

$$L_{sh} \sim 10^2 \frac{c}{\omega_{pi}} \qquad u_{sh} = 0.075\, c$$

$$k_\perp \sim \omega_{pi}/c \qquad \Rightarrow \boldsymbol{\nu_i \sim 10^{-4}\omega_{pi}}$$

AV, V. Tsiolis et al., PRL (2024)

Electron scattering frequency

Decorrelation of betatron oscillations

- Betatron deflection angle $\Delta\theta^2 \sim \omega_{\beta,e}^2\, r_\perp^2/u_{\mathrm{th}}^2$
- Crossing time of a disrupted filament $\Delta t \sim \dfrac{r_\parallel}{|u_{\mathrm{th}}|}$

~ Conserved canonical momentum

$\mathrm{l}_\parallel \sim |u_{th}|\Delta t$

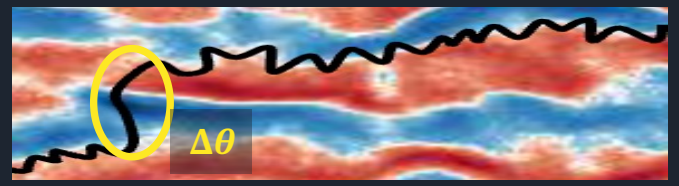

$$\nu_e \sim 2\pi \frac{k_\parallel}{k_\perp}\frac{m_i}{m_e}\frac{|u_{\mathrm{sh}}|}{r_{g,i}}$$

Longitudinal scale set by filament disruption

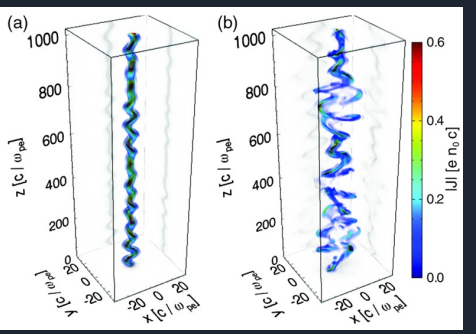

Ruyer & Fiuza, 2018

A Monte Carlo-Poisson approach to solve the coupled transport of electrons and ions in a decelerated microturbulence

Semi-dynamical approach to electron-ion transport

For a white noise with isotropic scattering, the transport equation reduces to

$$\dot{\boldsymbol{p}} = \underset{1.}{\boldsymbol{p} \cdot \boldsymbol{\delta\widehat{\Omega}_t}} + \underset{2.}{q\,\boldsymbol{E}} - \underset{3.}{m\,\dot{\boldsymbol{u}}_w}$$

1. **Pitch-angle scattering:** Gaussian white-noise process
Scattering center frame

$$< \delta\widehat{\Omega}_t > = 0 \qquad < \delta\widehat{\Omega}_t\, \delta\widehat{\Omega}_{t'} > = 2\,\delta(t' - t)$$

2. **Poisson solver**: self-consistent solution to the electrostatic field
Shock front frame

$$\nabla^2\phi = -4\,\pi\,\rho$$

3. Stationary scattering center frame deceleration // effective gravity

Free parameters: ν, L_{sh}

Automatically decompose the work from electric field:

- Monte Carlo ⇒ Motional electric field ($\sim E_\perp$)
- Poisson ⇒ cross shock potential ($E_\parallel$)

Coupled dynamics of electrons and ions:

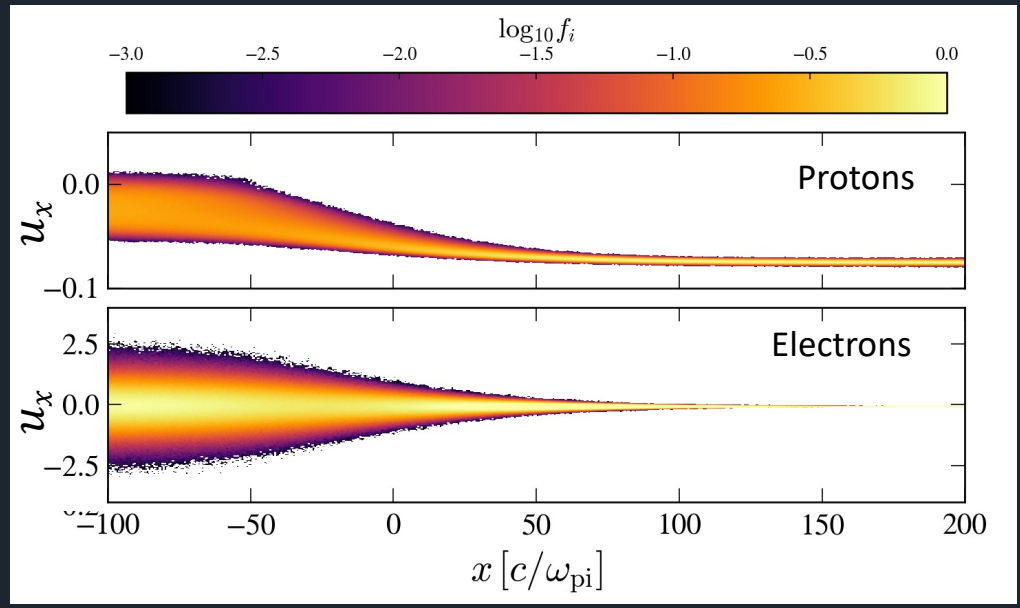

$$m_i = 1836\,m_i; v_i = \frac{|u_\infty|}{L_{sh}}; \nu_e = \frac{m_i \nu_i}{m_e}; L_{sh} = 150\,c/\omega_{pi}$$

AV, V. Tsiolis et al., PRL (2024)

The transport equation captures ambipolar electron heating and non-adiabatic ion heating in the decelerating turbulence

Particle-In-Cell

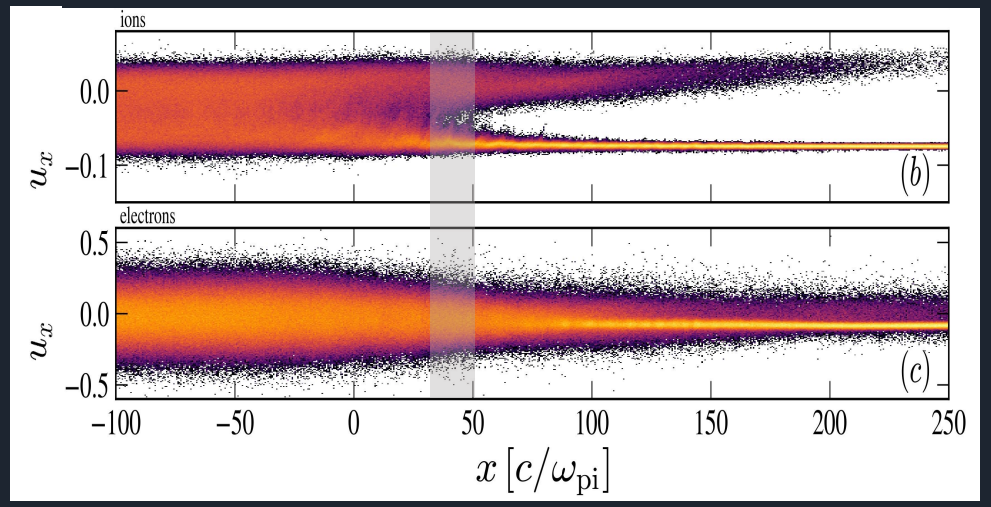

$u_{sh} = 0.075; \mathrm{m_i} = 49\ \mathrm{m_e}$ (**Tristan-mp**)

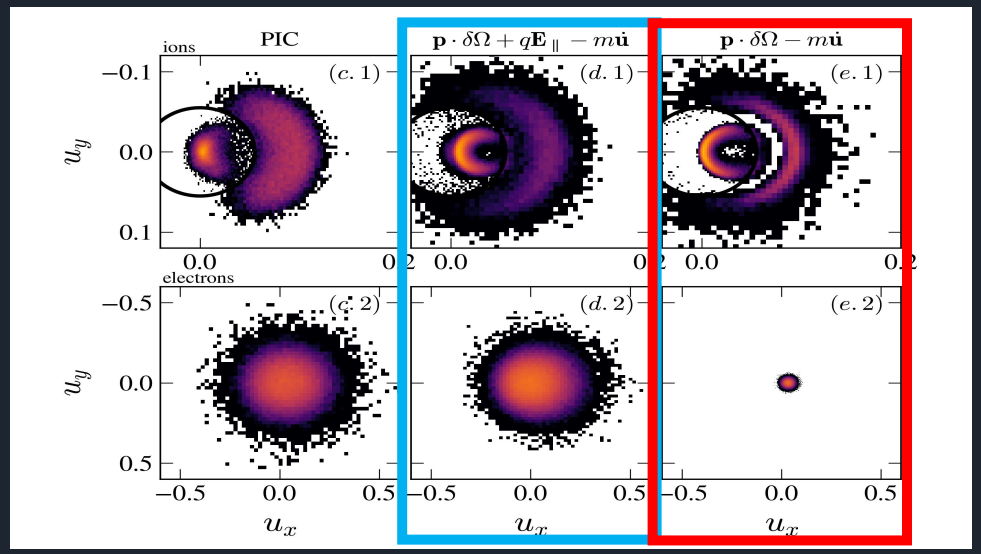

Theory

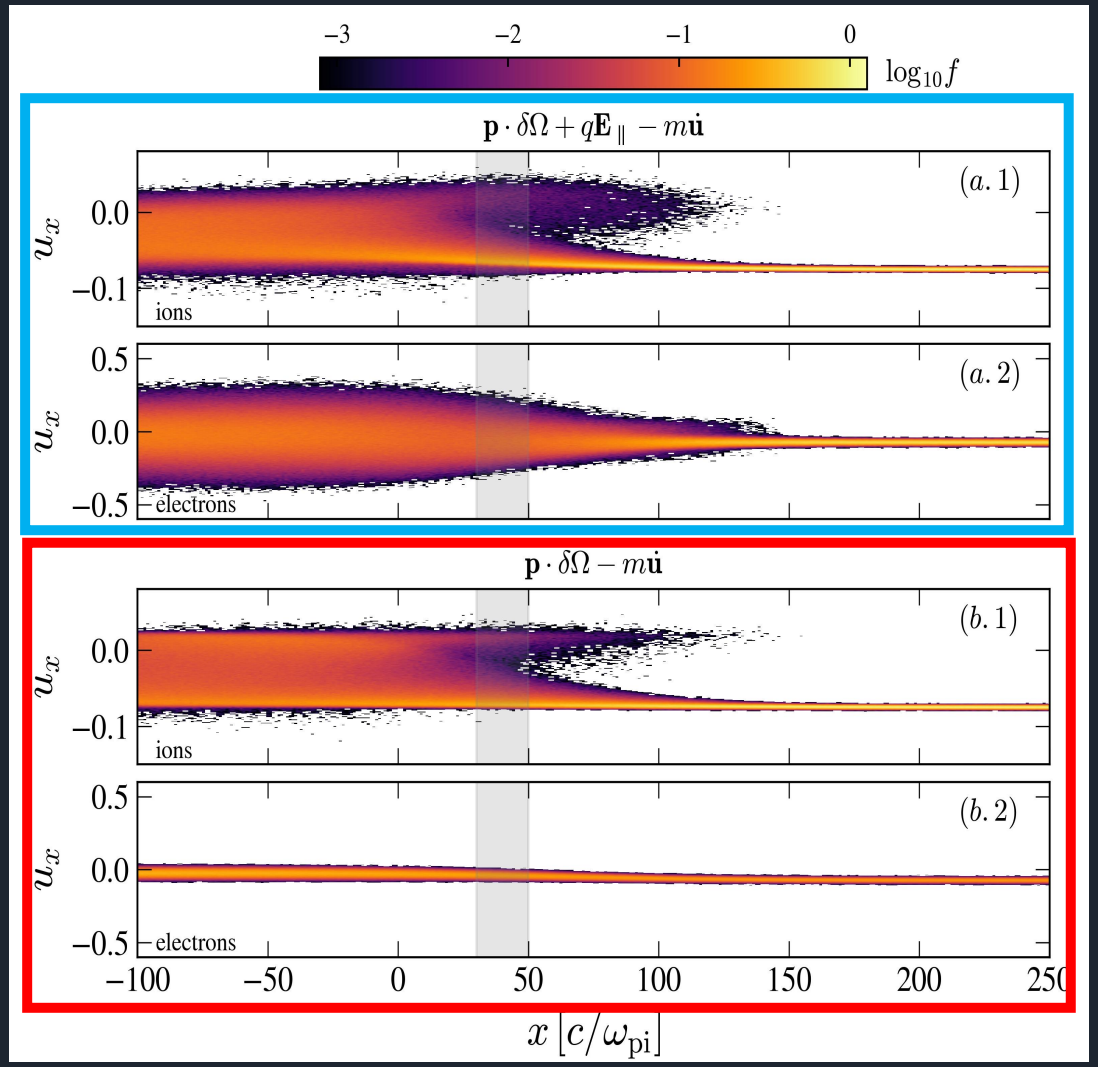

$m_i = 49\ m_i\ ;\ \nu_i = \frac{|u_\infty|}{L_{sh}}; \nu_e = \frac{m_i \nu_i}{m_e}; L_{sh} = 150\frac{c}{\omega_{pi}}$

AV, V. Tsiolis et al., PRL (2024)

Ambipolar heating in Weibel-mediated shock waves naturally leads to the expected energy partition

Moments of the transport equation in the diffusive regime ($f = f_0 + \mu\, f_1$)

$$\frac{1}{m_i}\,\partial_x\, P_e \simeq \frac{u_\infty}{u_w}\frac{j_\infty^2}{\phi_\infty}\frac{e^2 E_x^2}{\nu_e m_e u_w} \quad \Rightarrow$$

Joule-type heating in the ambipolar electric field: $eE_x \simeq \frac{3}{4\xi}\left(e^{\frac{\xi x}{L_{sh}}} - 1\right) m_e \nu_e u_\infty$

$\phi_\infty = m_i\, n_\infty\, u_\infty^2$

Heating rate

$$L_{sh}|\partial_x \tau^{xx}| = \phi_\infty \begin{cases} \frac{3}{16}\xi & \text{if } \xi \lesssim 1 \\ \frac{3}{4}\,\xi^{-1} & \text{if } \xi \gg 1 \end{cases}$$

Ambipolar parameter

$$\xi \sim \frac{m_e \nu_e}{m_i \nu_i} \sim k_\parallel\, r_{g,i} \sim 1$$

for a typical kink-driven filament disruption

- **Trapped electron/untrapped**
  ⇒ optimal electron heating
- Transition to **ion trapping** (Bell, merging, cavities, etc.) ensures efficient electron-ion energy partition

$$\Rightarrow \xi \sim \frac{m_e \nu_e}{m_i \nu_i} \sim 1$$

Downstream temperature ratio

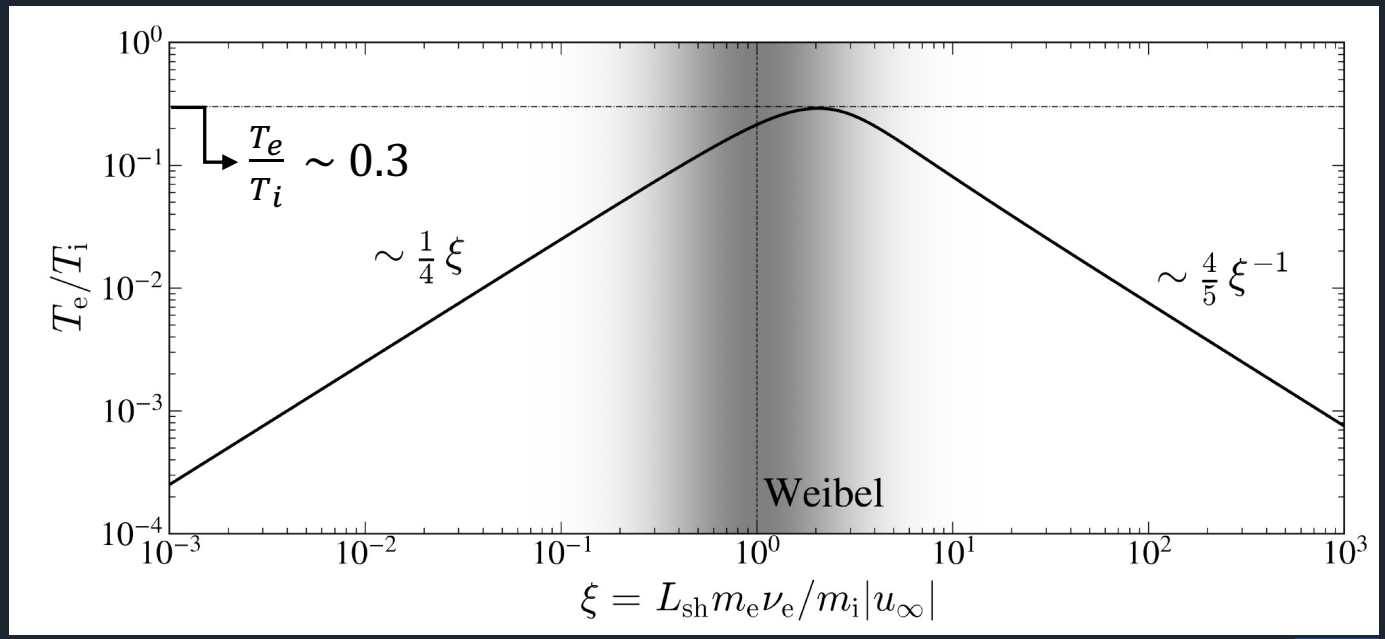

AV, V. Tsiolis et al., PRL (2024)

[a]AV, V. Tsiolis et al., submitted

Energy partition in transrelativistic shocks

PIC simulation of transrelativistic shocks
from $u_{sh} = 0.075$ to $u_{sh} = 173$

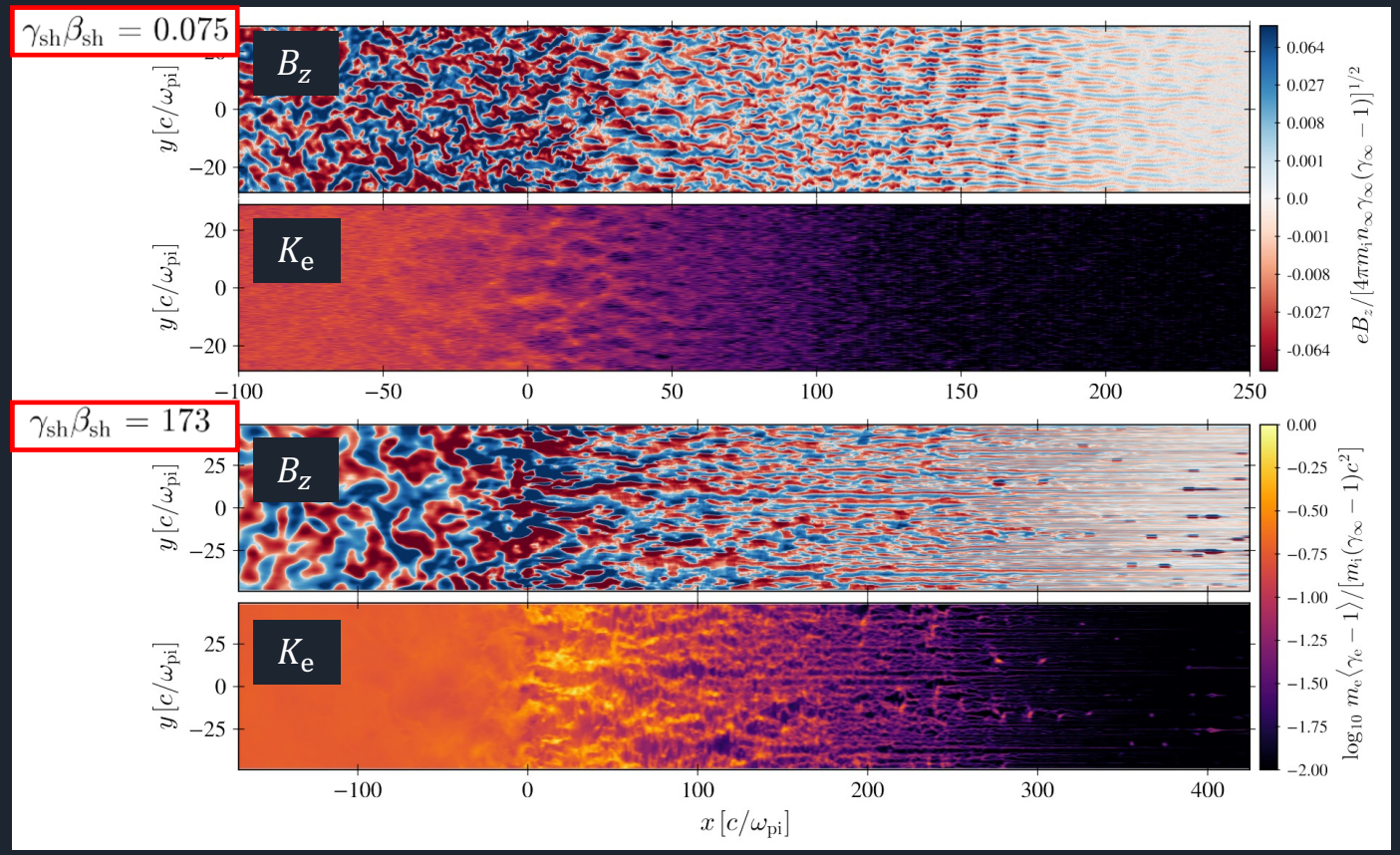

AV et al., submitted

Equipartition between electrons and ions is observed in the ultra-relativistic regimes of Weibel-mediated shocks

$\gamma_{sh} = 1/\sqrt{1-\beta_{sh}^2}$

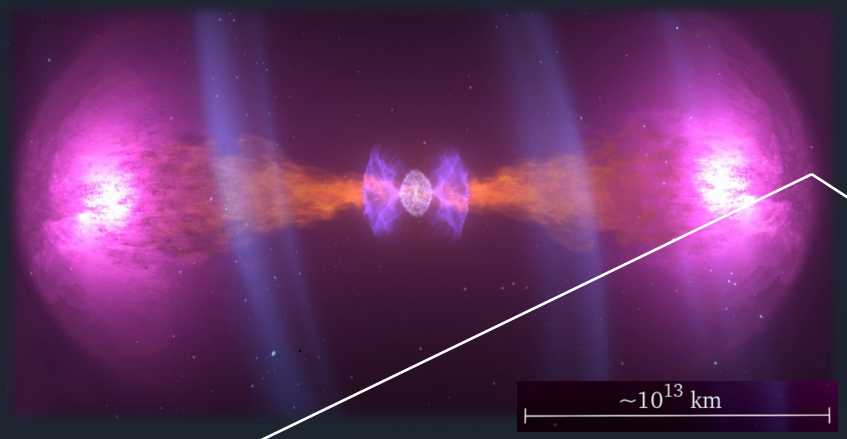

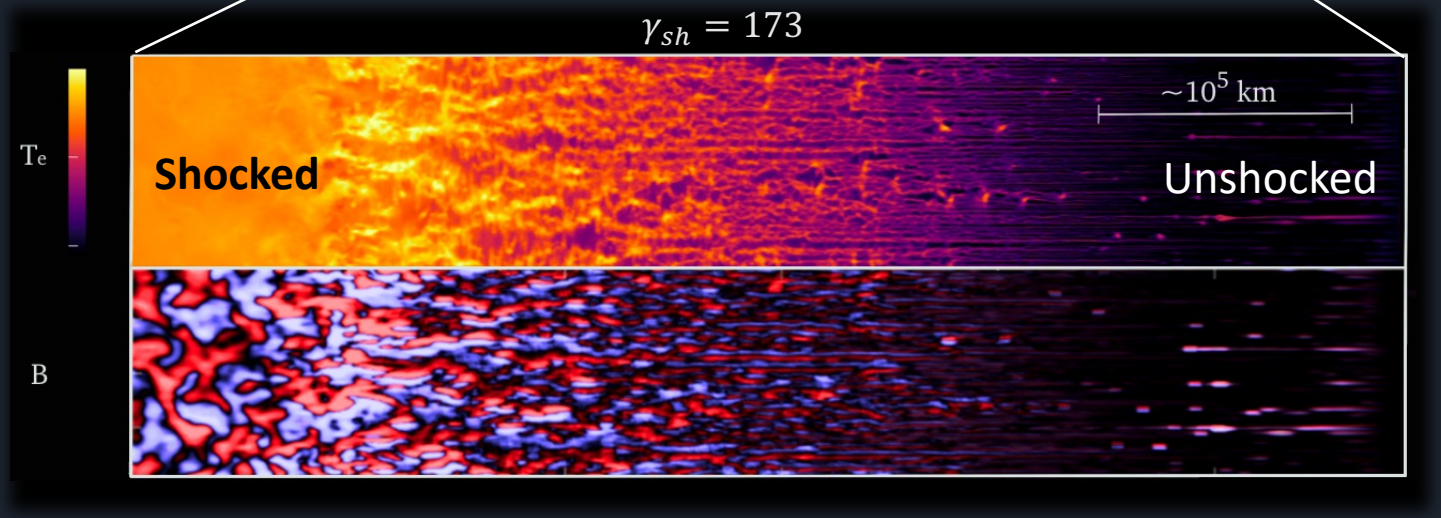

Particle-In-Cell simulation – (top) Temperature; (bot) B-field

AV, Lemoine, Gremillet, ApJL 2022

Relativistic Weibel-mediated shocks efficiently heat the electrons up to close to equipartion, leading to efficient electron injection

$$E_e \sim E_i \Rightarrow \langle \gamma_e \rangle \sim \frac{m_i}{m_e} \langle \gamma_i \rangle \sim 10 \text{ GeV}$$

- Modeling of gamma-ray burst emission[1]
- In kinetic simulations[2,3,4]

$$\frac{T_e}{T_i} = 0.45 - 0.5$$

Mean kinetic energy per particle

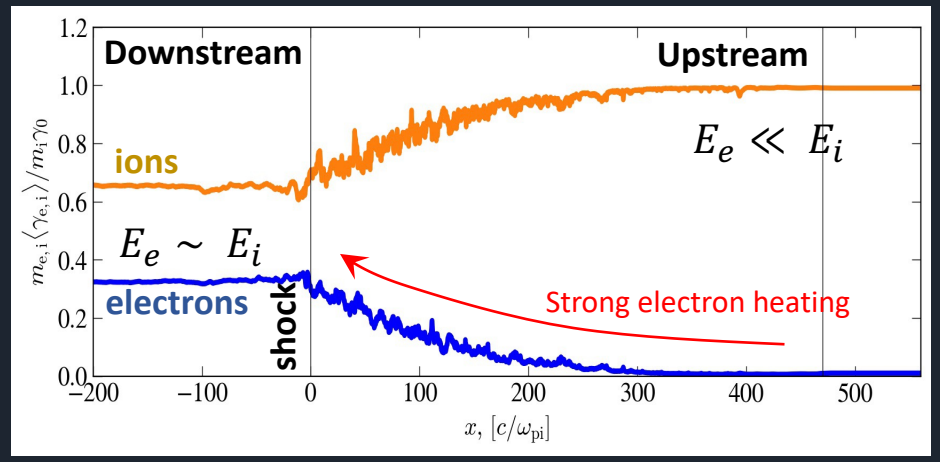

$\frac{m_e}{m_i} E_i$

AV, Lemoine, Gremillet, ApJL 2022

[1]D. Freedman, E. Waxman ApJ 547, 192 (2001)

[2]A. Spitkovsky, ApJL 673, L39 (2008)

[3]S. Martins et al., ApJL 695, L189 (2009)

[4]T. Haugbolle, ApJL 739, L42 (2011)

Generalizing the picture to transrelativistic shocks

A constant electron temperature points toward generality of the heating mechanism and weak sensitivity to details of the microturbulence

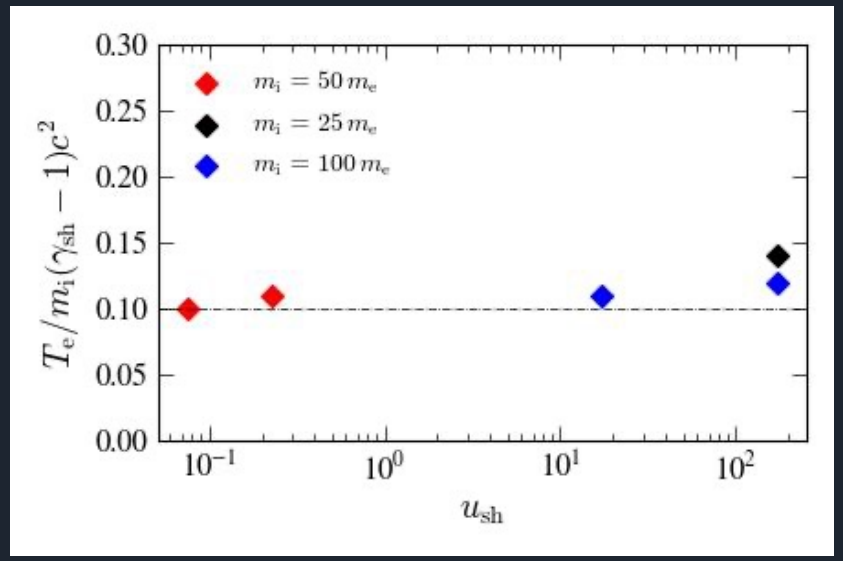

- Systematic electron heating up to

$$T_e = 0.1\,(\gamma_{sh} - 1)m_i c^2$$

- In terms of temperature ratio

$$\frac{T_e}{T_i} \sim \mathbf{0.3} \text{ for } u_{sh} \ll c$$

$$\frac{T_e}{T_i} \sim \mathbf{0.5} \text{ for } u_{sh} \gg c$$

The theory naturally generalizes to the relativistic regimes

$$\nu^{trapped} = 2\,\pi \frac{r_\perp}{r_\parallel}\,\epsilon_B^{1/2}\left(\frac{p_{|w}}{m_i c\sqrt{\gamma_{sh}-1}}\right)^{-1}\beta_{|w}\,\omega_{pi} \propto \frac{\epsilon_B^{1/2}}{\gamma_{|w}}$$

$$\nu^{untrapped} = \frac{\omega_{pi} r_\perp}{c}\,\epsilon_B\left(\frac{p_{|w}}{m_i c\sqrt{\gamma_{sh}-1}}\right)^{-2}\beta_{|w}\,\omega_{pi} \propto \frac{\epsilon_B}{\gamma_{|w}^2}$$

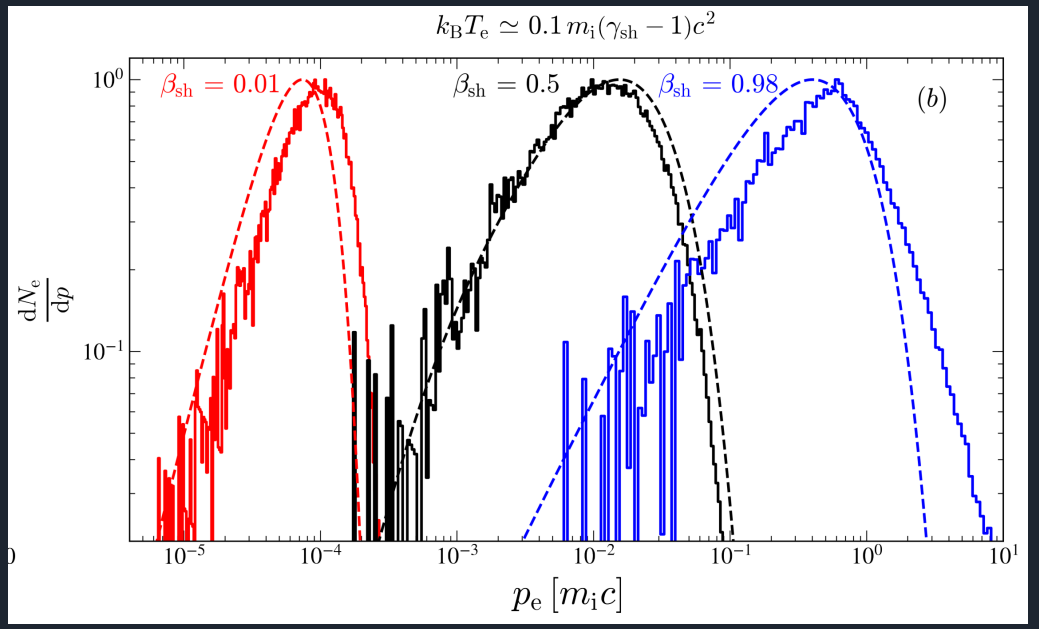

Fokker-Planck solution

AV et al., submitted

The ambipolar electric field also accounts for the electron dynamics in the relativistic regime

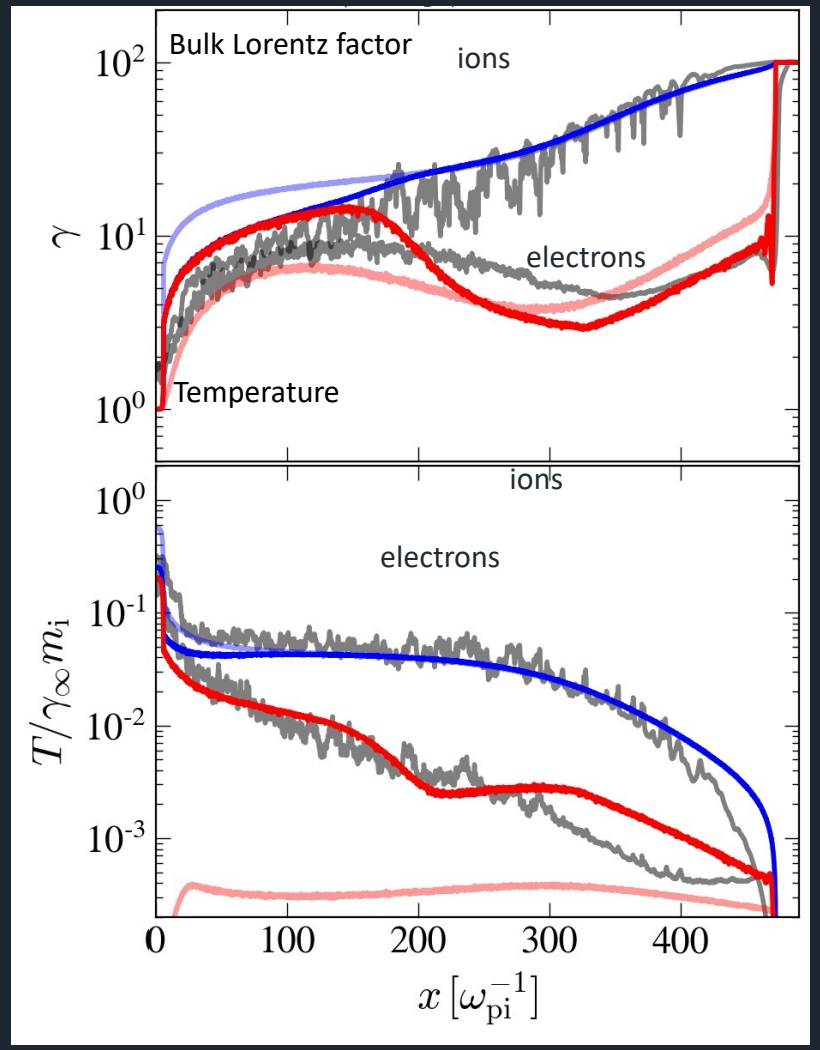

Blue/**Red** : Reconstructed trajectories of ions and electrons from the transport equation

PIC
Theoretical model
- **ions**
- **electrons**

Light red: T_e from theoretical model in **absence of longitudinal electrostatic field**

⇒ Pure pitch-angle scattering cannot explain equipartition.

Red : T_e from theoretical model **with longitudinal electrostatic field**

⇒ Overall, satisfactory reconstruction of velocity and temperature, with electron heating up to equipartition

AV, Lemoine, Gremillet, ApJL 2022

Particle acceleration and formation of a nonthermal tail?

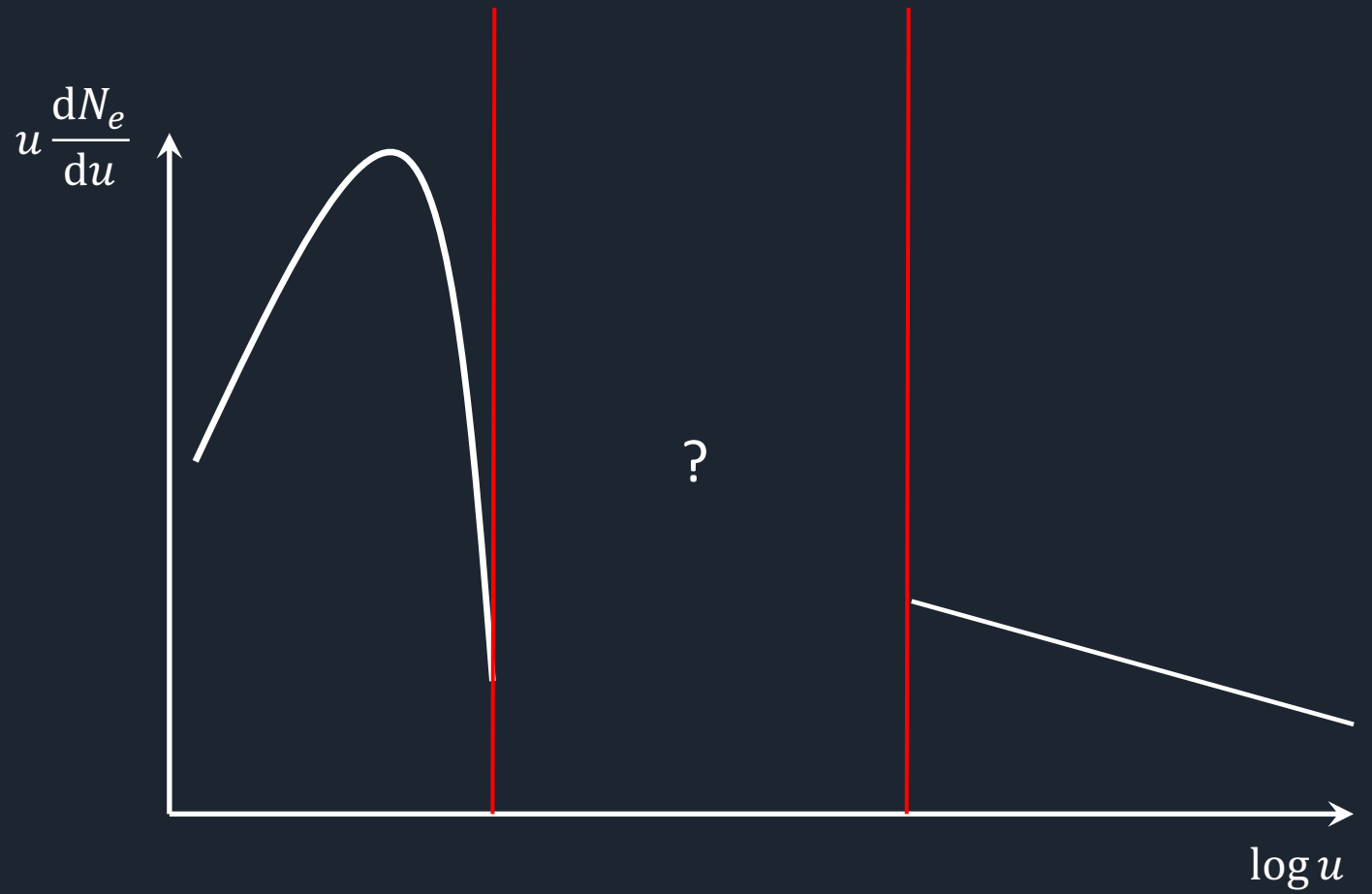

Reasonable values of the Weibel-mediate coherent electrostatic field are sufficient to accelerate electrons via Fermi process

Thermalization and acceleration

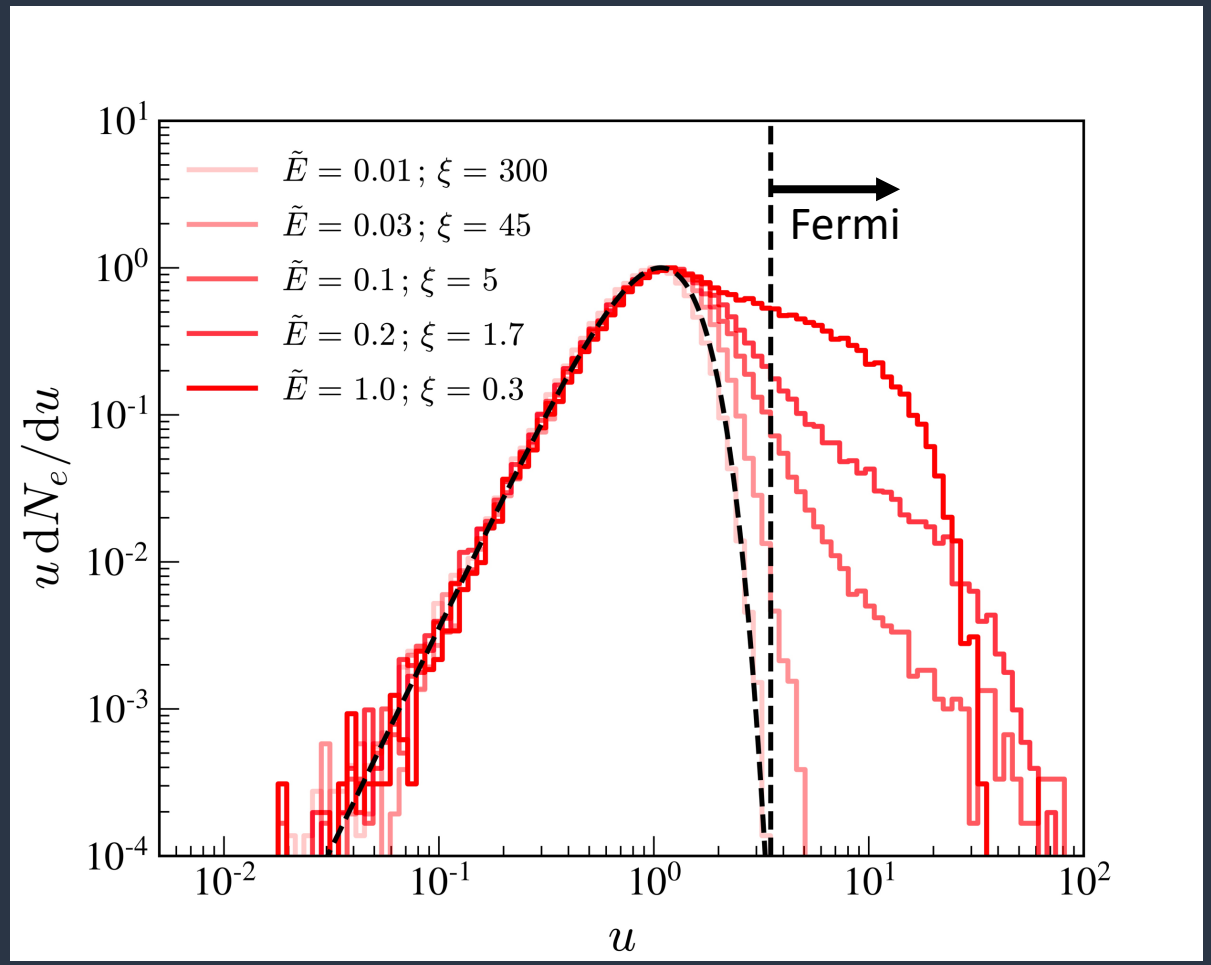

Dimensionless Fokker-Planck

Bulk heating — Fermi acceleration

$$\frac{\mathrm{d}}{\mathrm{d}\tilde{t}_{|w}} f = \frac{1}{\tilde{u}^2}\partial_{\tilde{u}}(D_{\tilde{u}\tilde{u}}\,\tilde{u}^2\,\partial_{\tilde{u}}\,f) + \frac{2}{3}\,\tilde{u}\,\frac{q}{e}\,\tilde{E}\,\partial_{\tilde{x}}\,\tilde{u}\,f + \partial_x D_{\tilde{x}\tilde{x}}\,\partial_x\,f$$

$$D_{\tilde{u}\tilde{u}} = \frac{1}{3}\,\tilde{E}^2 \qquad D_{\tilde{x}\tilde{u}} = \frac{2}{3}\frac{q}{e}\tilde{E}\,\tilde{u} \qquad D_{\tilde{x}\tilde{x}} = \frac{1}{3}\tilde{u}^2$$

$$\tilde{E} = \frac{eE}{m_e\,\nu_e\,|u_\infty|} \qquad \xi = \frac{\nu_e\,m_e\,L_{sh}}{m_i|u_\infty|}$$

Fraction of suprathermal electron

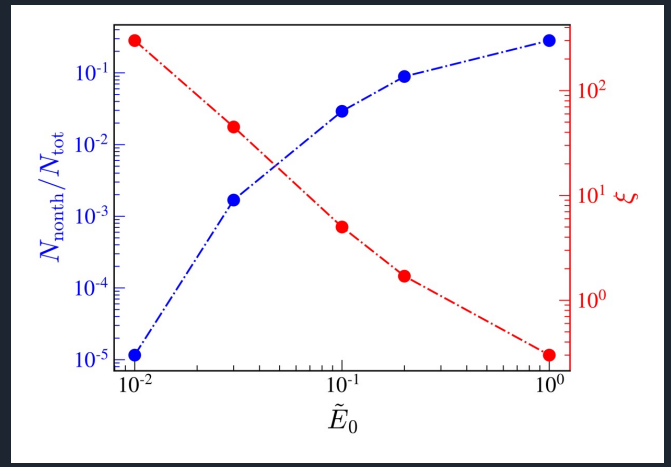

To conclude…

In short

Heating results from the ambipolar electric field that accelerates electrons, which are thermalized by rapid scattering in the Weibel-mediated turbulence.

Energy partition peaks around Te/Ti $\sim$ 0.3 with a weak dependence on higher-order effects in the statistics of electron transport and nonlinear dynamics of the instability.

Successive nonlinear modes resulting in ion trapping naturally lead to $\xi \sim 1$

The model extends to transrelativistic shocks with systematic efficient electron heating up to $T_{\mathrm{e}} = 0.1\ (\gamma_{\mathrm{sh}} - 1) m_{\mathrm{i}} c^2$

The ambipolar electric field can serve as a startup mechanism for electron injection in the classical regime together with spatial diffusion in the velocity gradient of the scattering center frame

The turbulence is magnetically dominated, and drifts close to the electron bulk velocity

Background plasma parameters

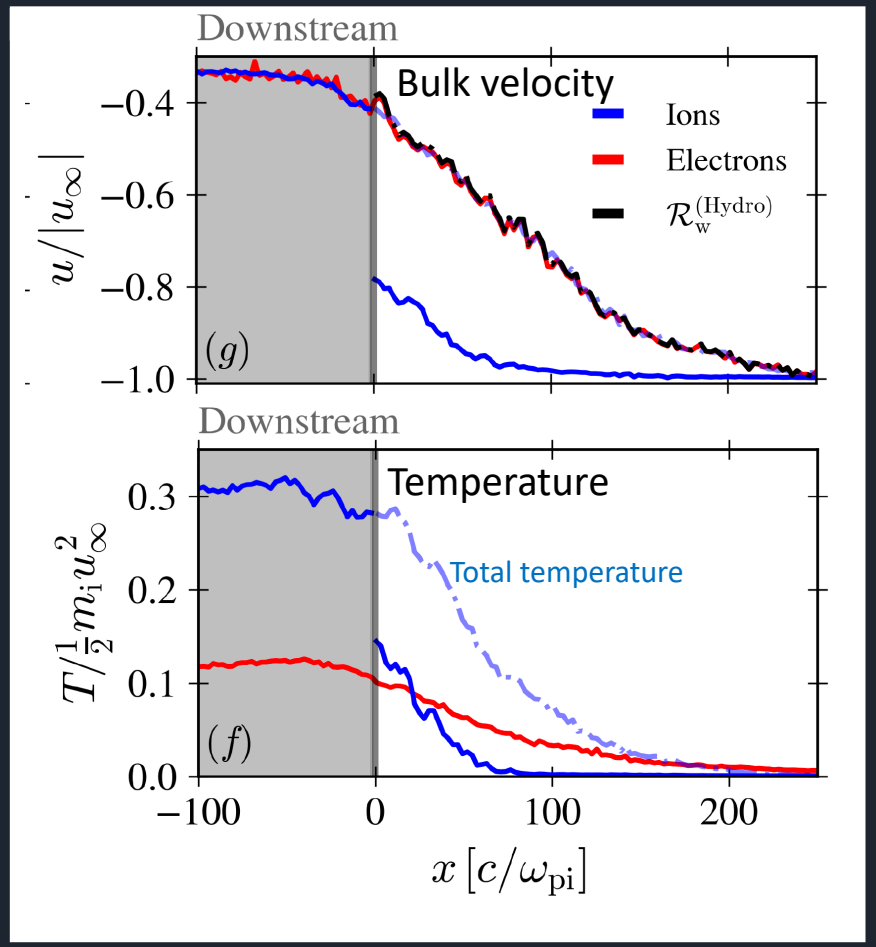

A natural scattering center frame: the Weibel frame

- The precursor of the shock is dominated by the Weibel instability

$$\Rightarrow \boldsymbol{E}^2 - \boldsymbol{B}^2 < 0$$

- At each point, one can define a local quasi-magnetostatic reference frame $\mathcal{R}_w$ [1,2]

$$\Rightarrow u_w \sim \frac{E\times B}{B^2} \sim \frac{\omega}{k}\frac{\epsilon_{xy}}{\epsilon_{yy}} \sim u_e$$

- Electrons drift close to the Weibel frame in the shock precursor

[1]C. Ruyer et al PRL 117, 065001 (2016) [2]G. Pelletier et al PRE 100, 013205 (2019)

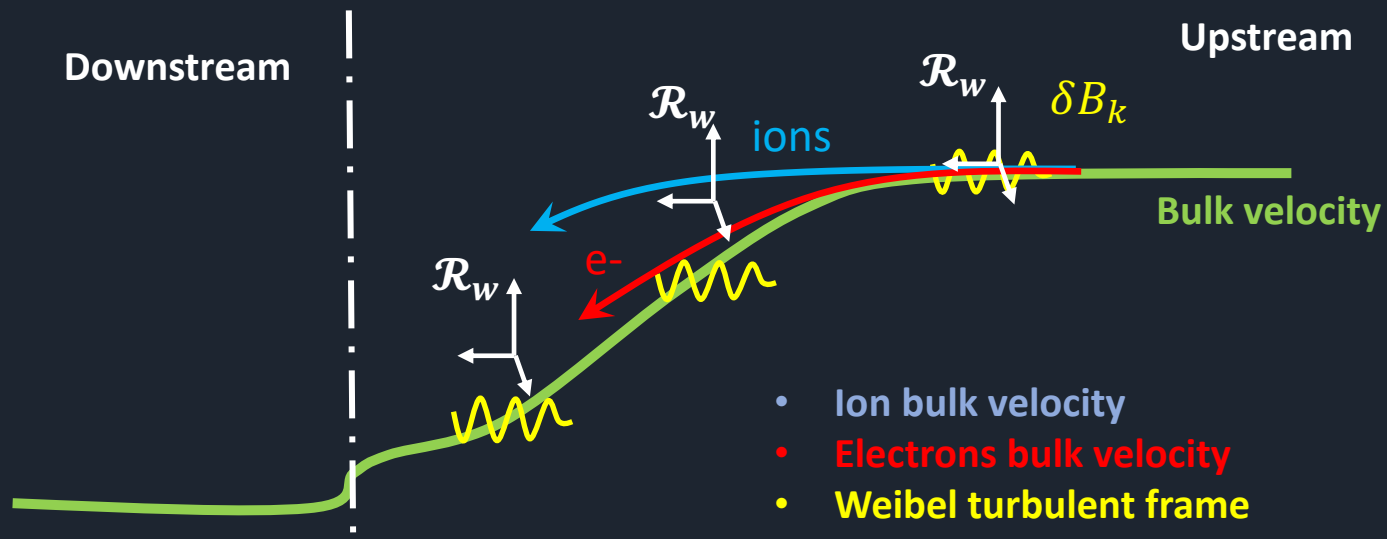

[a]AV, V. Tsiolis et al., submitted

In the relativistic regime, the energy dependence of the scattering frequency is important to account for equipartition

The model extends to the relativistic regime of turbulent deceleration

$$\dot{\boldsymbol{p}}^i = \left(\boldsymbol{p}\cdot\delta\widehat{\boldsymbol{\Omega}}_t\right)^i - \Gamma^i_{ab}\,p^a\,\beta^b + q\,E_\parallel$$

⇒ Linear Fokker-Planck equation

$$\sim \partial_x f + \cdots \frac{du_w}{dx}\,\partial_p f\, + \cdots \partial_p\left(D_{pp}\,\partial_p f\right) = 0$$

$$D^e_{pp} \propto \frac{1}{\nu}\left(\frac{2}{3}\frac{du_w}{dx} + \frac{q\,E_\parallel}{p}\right)^2 \sim \frac{1}{\nu}\left(\frac{q\,E_\parallel}{p}\right)^2$$

For E ~ 0, heating is analogous to shearing acceleration

$$D_{pp} \propto \frac{1}{\nu}\left(\frac{du_w}{dx}\right)^2$$

The scattering frequency of the electron varies by order of magnitude from the far upstream to the shock transition

$\lambda \sim d_e \sim d_i$ ⟵ $\lambda \sim d_e$

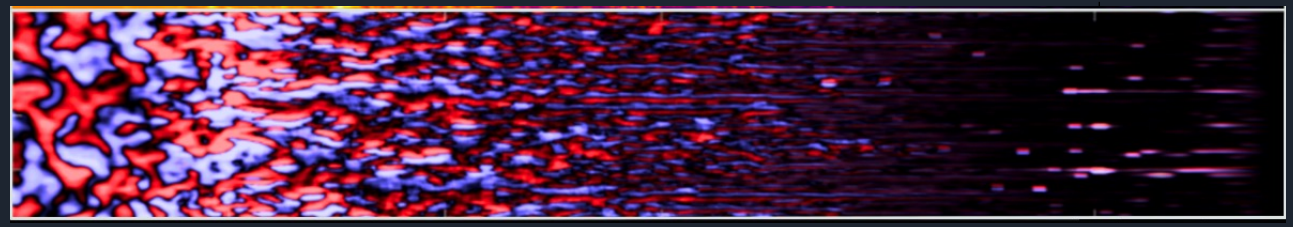

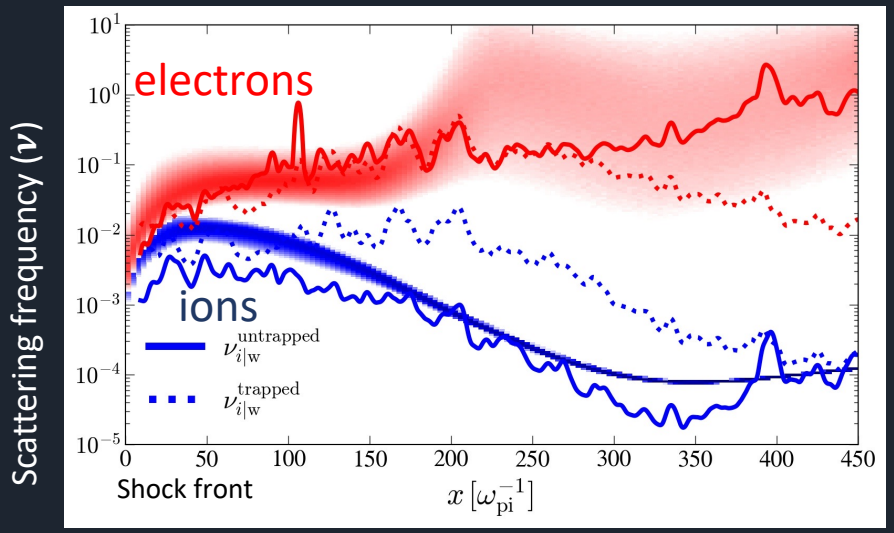

AV, Lemoine, Gremillet, ApJL 2022